energies

MDPI

Article

Impact of Reactive Power from Public Electric Vehicle Stations on Transformer Aging and Active Energy Losses

Ana Pavlićević * and Saša Mujović

Faculty of Electrical Engineering, University of Montenegro, Džordža Vašingtona bb, 81000 Podgorica, Montenegro

* Correspondence: anaz@ucg.ac.me; Tel.: +382-67559535

Abstract: Climate change at the global level has accelerated the energy transition around the world. With the aim of reducing CO_2 emissions, the paradigm of using electric vehicles (EVs) has been globally accepted. The impact of EVs and their integration into the energy system is vital for accepting the increasing number of EVs. Considering the way the modern energy system functions, the role of EVs in the system may vary. A methodology for analyzing the impact of reactive power from public electric vehicle charging stations (EVCSs) on two main indicators of the distribution system is proposed as follows: globally, referring to active power losses, and locally, referring to transformer aging. This paper indicates that there is an optimal value of reactive power coming from EV chargers at EVCSs by which active energy losses and transformer aging are reduced. The proposed methodology is based on relevant models for calculating power flows and transformer aging and appropriately takes into consideration the stochastic nature of EV charging demand.

Keywords: electric vehicles; electric vehicle charging stations; active power losses; power distribution transformers; thermal aging; reactive power

Citation: Pavlićević, A.; Mujović, S. Impact of Reactive Power from Public Electric Vehicle Stations on Transformer Aging and Active Energy Losses. *Energies* **2022**, *15*, 7085. https://doi.org/10.3390/en15197085

Academic Editor: Wojciech Cieslik

Received: 16 August 2022
Accepted: 21 September 2022
Published: 27 September 2022

1. Introduction

In July 2009, the leaders of the European Union and the G8 announced the aim to reduce greenhouse gas emissions to at least 80% below 1990s' levels by 2050. The automotive sector has a very important role to play in achieving this ambitious goal [1].

One of the best ways to promote the use of electric vehicles (EVs) is to increase the number of available public electric vehicle charging stations (EVCSs). Connecting a large EV fleet in a small area faces a number of challenges such as: overheating distribution transformers, increasing power losses, voltage instability and harmonic distortion [2,3]. Therefore, there is a need for modeling and mitigating the impacts of EVCSs on the distribution grid. Connecting EVCSs to the distribution system has a significant impact on the exploitation of the existing energy infrastructure. This especially refers to increasing the total load, peak load and changing the load profile of the distribution transformer where EVCSs are connected. Taking into account a large number of distribution transformers as well as the fact that in most cases they do not operate in parallel in low voltage networks, the prevention of failures or possible losses of life (LOL) is of great importance. Since charging EVs at EVCSs increases load on distribution transformers, it could cause overloading and therefore overheating of distribution transformers. Apart from overheating, there are other sources of transformer aging such as: fault currents caused by short-circuits or inrush currents, overvoltage caused by lightning and switching impulses, contamination of the oil that could shorten their lifetime and cause premature failure [4,5]. Bearing in mind that the subject of this paper is the influence of EVCS on the power system and on transformer aging under normal operating conditions, an overview of the literature related to the aging of transformers under such conditions is given.

Researches have studied the impact of distributed generation (DG) and energy storage (ES) on transformer aging [6,7]. It has been concluded that with a high penetration of

EVs, and no support from photovoltaic (PV) and ES, the transformers will dramatically age. Furthermore, researchers have dealt with the influence of the charging method on transformers' aging [8–13]. The main idea is to find an optimal charging scheme to minimize the impact of EVs' charging demand on distribution transformers. The [8] proposed model considers time-of-use rates in order to minimize energy consumption costs and avoid transformer overloading and LOL based on load and meteorological data. The proposed smart charging scheme together with PV with ES can prevent transformer overloading and LOL. PV generation can reduce the energy purchased from the grid, while ES can assist during peak hours. Three smart ways of charging (central, decentralized and hierarchical) as well as dump charging have been analysed [9]. Based on the obtained results, it has been concluded that hierarchical charging strategies are the most desirable in terms of LOL, while the centralized charging strategy (valley filling) has shown the greatest LOL of transformers. In one paper [10], a simple method is used to coordinate the charging process of PEVs to avoid the overloading of transformers by using the fact that idle time represents a significant percentage of EV parking time. In the paper, [11] reducing the impact on transformer aging by implementing the capability of delivering a variable charging rate has been proposed. Two charging algorithms have been used as strategic ways for reducing the overload of distribution transformers. The results suggest that for both uncontrolled and controlled charging, the load on the transformer will be reduced. Since the current commercial, residential charging technology is categorized, infrastructure changes are necessary in order to support this idea. Another paper [12] proposes a temperature-based smart charging strategy that reduces transformer aging without substantially reducing the frequency by which EVs obtain a full charge. These reductions are substantially larger at hot climate locations compared to cool climate ones. The results indicate that simple smart charging schemes, such as delaying charging until after midnight can actually increase, rather than decrease, transformer aging. The authors of [13] analyze the impacts of a price incentive-based demand response on neighburhood distribution transformer aging. The results indicate that the integration of EVs in residential premises may indeed cause accelerated aging of distribution transformers, while the need to investigate the effectiveness of dynamic pricing mechanisms is evident. In [14], the number of EVs has been optimized by calculating additional steady-state hottest-spot temperature rises by ensuring that distribution reliability requirements are met.

In order to reduce transformer aging, the reactive power potential from on-board EV chargers (OBCs) at EVCSs is proposed in this paper. OBCs in modern EVs are bidirectional, which allows them to work in all four quadrants [15]. Using reactive power support, as a part of the vehicle-to-grid concept, is already familiar and has been investigated as, e.g., part of on-line control for improving the voltage stability of a microgrid with PV, wind, battery storage, residential and commercial building feeders [3], the load control of active and reactive power [16], the compensation of reactive load of wind turbines near the station [17] and the revenue potential of providing reactive power service [18]. In this paper, the respective value of reactive power is obtained by small oversizing charging converters, which does not require an upgrade of the charging infrastructure. In relation to [15], where the influence of the oversizing of converters on voltage deviations, peak load and grid losses in the network has been analyzed, this paper's analysis is extended to include transformer aging. Besides the impact on transformer aging, also the influence of reactive power potential of EVCSs is analyzed with the aim of reducing active energy losses without additional devices and facilities. Locations of EVCSs are chosen from the aspect of increasing the efficiency of the network, which refers to reducing total active energy losses.

The reduction of losses in the power system in the presence of EVCSs is achieved in different ways. A large number of papers can be found in the literature that treat the problem of reducing energy losses in the presence of electric vehicles, e.g., optimal operation of vehicles with distributed generators [19–23], optimal reconfiguration of the distribution network [24–28], optimal operation of the battery storage, [29,30], optimal charging strategies [31–34] and optimal location and size of reactive power compensators [35,36].

The contribution of this paper is related to the impact analysis of the influence of reactive power on active power losses and transformer aging. In other words, the paper proposes a methodology that allows the determination of the optimal injection of reactive power of the EVCSs with the aim of reducing transformer aging and reducing active power losses. The proposed method is based on the well-known model for calculating transformers' aging, which is described in detail in [37]. It is applicable to an arbitrary network with an arbitrary number of EVCSs. Considering the stochastic nature of EV charging demand, the presented paper clearly indicates the benefits and limitations of reactive power from OBCs at EVCSs to energy losses reduction and transformers aging.

Numerical results, obtained in MATLAB and on the IEEE 33 bus radial distribution network, indicate that it is possible to achieve the optimal value of injecting reactive power from EV vehicles in order to enable reductions of transformers' aging and a reduction in energy losses in relation to the case where there is no reactive power injection or when reactive power injection is the maximum possible. This analysis may serve focus on local distributions in order to prevent shortening transformers' working life. Furthermore, the presented results may be useful for the analysis of global distribution system parameters such as energy losses and node voltages.

The rest of the paper is organized as follows. Section 2 is dedicated to the system components modeling. In Section 3, a description of methodology is given, while in the final Section 4, the most important conclusions and directions for further research have been stated.

2. Modeling System Components

2.1. Load Modeling

There is certain number of load models in the literature that can be used for various analyses. In addition, in recent times, new nodal classifications have been made and their characteristics have been reviewed [38]. Considering that a steady state analysis is performed in this paper, basic information about node loads have been used in this paper. Namely, loads in the system are modeled as PQ nodes. On the basis of the type of loads connected to the nodes busses, three types have been adopted: residential, commercial and industrial busses, as seen in Table 1 [19]. There are 18 residential busses, 5 commercial buses and 9 industrial buses. Load changing over time has been taken into account by introducing a load scaling factor. Load scaling factor changes over time as a percentage of nominal load, which varies depending on a load type, Figure 1, [39].

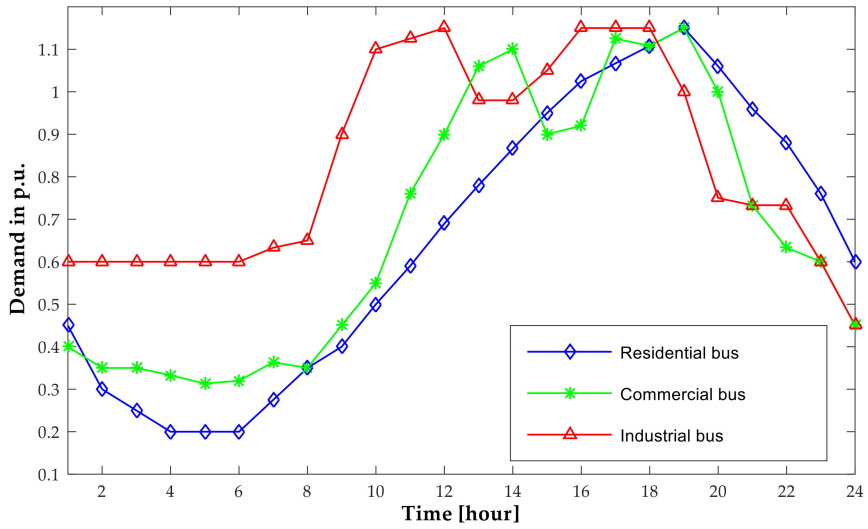

Figure 1. Typical buses load curve, [39].

Table 1. Grouping of buses data, [19].

Bus Type	Bus Numbers
Residential	2, 3, 5, 6, 7, 8, 9, 10, 13, 14, 15, 16, 17, 20, 21, 23, 24, 25
Commercial	4, 11, 12, 18, 19
Industrial buses	22, 26, 27, 28, 29, 30, 31, 32, 33

2.2. Public EVCS Modeling

According to the way EVs are connected to the electric grid, there are two types of charging strategy: conductive EV charging and inductive EV charging. In conductive charging, there is a physical connection between EV and the electrical grid. In inductive charging, also known as wireless power transfer [40], there is no galvanic connection between the vehicle and the electrical grid. Since conductive charging is the most common method of charging, this type of charging has been analyzed. There are two types of conductive charging in EVCSs: AC charging and DC charging with different power levels: Level 1, Level 2 and Level 3 charging. In this paper, the AC Level 2 type of charging station has been analyzed because of its simple infrastructure, low price and availability for the most commercial types of charging in public places.

There is a certain number of models for grid support by EVCSs [41]. Bearing in mind that vehicles are mostly stationary during the day, their role may be different. The literature recognizes that EVCSs could most effectively serve in the following ways: to ensure a fast frequency response [42,43] for shifting electricity [44,45], improve power quality [46] and as energy storage [44].

Significant work has been done towards minimizing grid losses due to PHEV charging through efficient charging algorithms with different objective functions [47–49]. All mentioned papers, in one way or another, with different stimulation techniques, have an influence on drivers' behavior. Nevertheless, this paper adopts an approach that does not impair the comfort of EV users, which means that two cases have been observed, which are as follows: active power is consumed during the charging of EVs; while in the second case, while charging with active power, vehicles inject reactive power.

2.2.1. Operation Region of EV Chargers

In order to obtain reactive power and not to jeopardize EVs drivers' habits, the concept of small oversizing of 5.3% of on-board chargers ratings has been used, [15]. With this, a significant amount of reactive power which is 32.9% of active power is obtained. What is important is that this does not require an upgrade of the charging infrastructure, and charging active power is the same in both cases. The operating region of on-board charger charging is region IV, Figure 2. It can be seen that with small oversizing of an EV charger, in Figure 2 shown as a larger circle, with the same active charging power, a representative value of reactive power is obtained.

The charging operation in the second and third quadrants of the P-Q diagram was not considered, since the management of the active power of the chargers affects the convenience of the consumers themselves as well as battery life. Furthermore, the operation of chargers in the first quadrant, wherein EV can also consume reactive power, is not suitable for the analyzed network and loads.

During the charging of EVs, we have analyzed the influence of reactive power from equal to zero to the maximum available. The national network operator in our country does not yet support the injection of active power or the injection and absorption of reactive power by the EVCSs. The operation of chargers in all four or two quadrants is discussed in the literature at the level of conceptual solutions for which there are numerical or real experiments. The results obtained both in this work and in the literature represent guidelines for changing the network requirements of new electricity consumers/producers. This paper demonstrates the benefits of reactive power from EV charger compared to the current regulation, which stipulates that they only consume active power. Finally, it is

important to note that the network codes for the LV network, after looking at the possible positive impact of the operation of network inverters of photovoltanic power plants, have been changed in Germany. For example, in Germany, LV grid-connected PV installations rated above 3.68 kVA have to follow a specified PF droop curve as a function of their instantaneous power output [15].

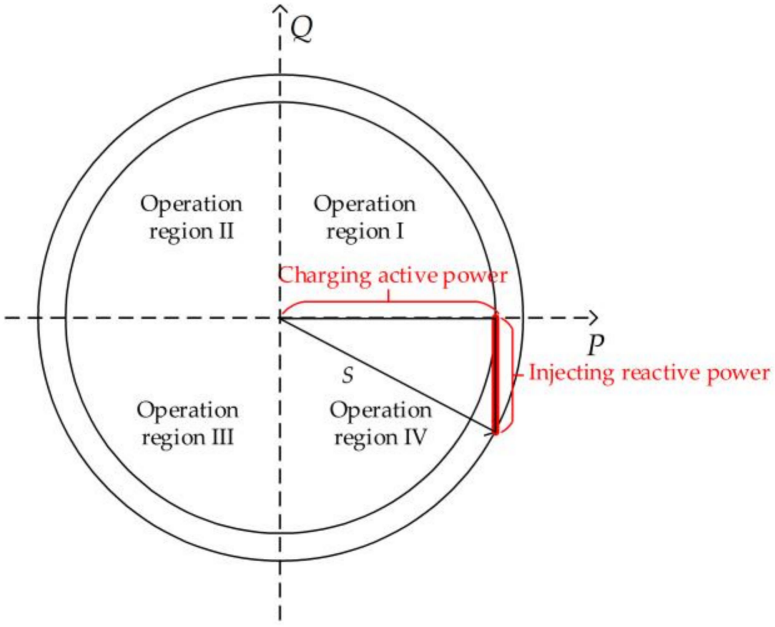

Figure 2. Operation region of EVs chargers.

Furthermore, it is very important to regulate the interaction between EVs the and distribution system. The design of the battery charger will be crucial in this effort to effectively control the power flows. One of the important requirements of an EV charger is the amount of current distortion that it draws from the grid [50]. Parameters such as total harmonic distortion (THD) and total demand distortion (TDD) can be used to evaluate the harmonic content of the charger. Additionally, the chargers should meet the individual harmonic limits as well [50–52]. The tasks of OBC system controller is to follow the charging power and reactive power commands controlled by the grid operator. In [50], the proposed design of OBC has shown analytically and experimentally that chargers are able to symmetrically operate at all four quadrants of the power plane. Furthermore, grid current requirements such as that the ac-dc converter input current THD should be limited to 5% have been satisfied.

Figure 3 shows the proposed application of on-board EV chargers used in this paper. The chargers form EVCS injecting reactive power at the point of common coupling (PCC) and decreases transformer overloading. In the case of the AC charging station, electric vehicle supply equipment (EVSE) serves for monitoring, management and communication with a vehicle during charging, while energy conversion from AC to DC power is suitable for charging battery performed via OBC.

In this paper, it is assumed that the power factor management of EVCSs is performed based on the previous day's consumption forecast of the analyzed network and EVCS demand. After processing the necessary data, the distribution network control centre sends a signal for the value of the power factor of the station. The power factor is constant during the 24 h period.

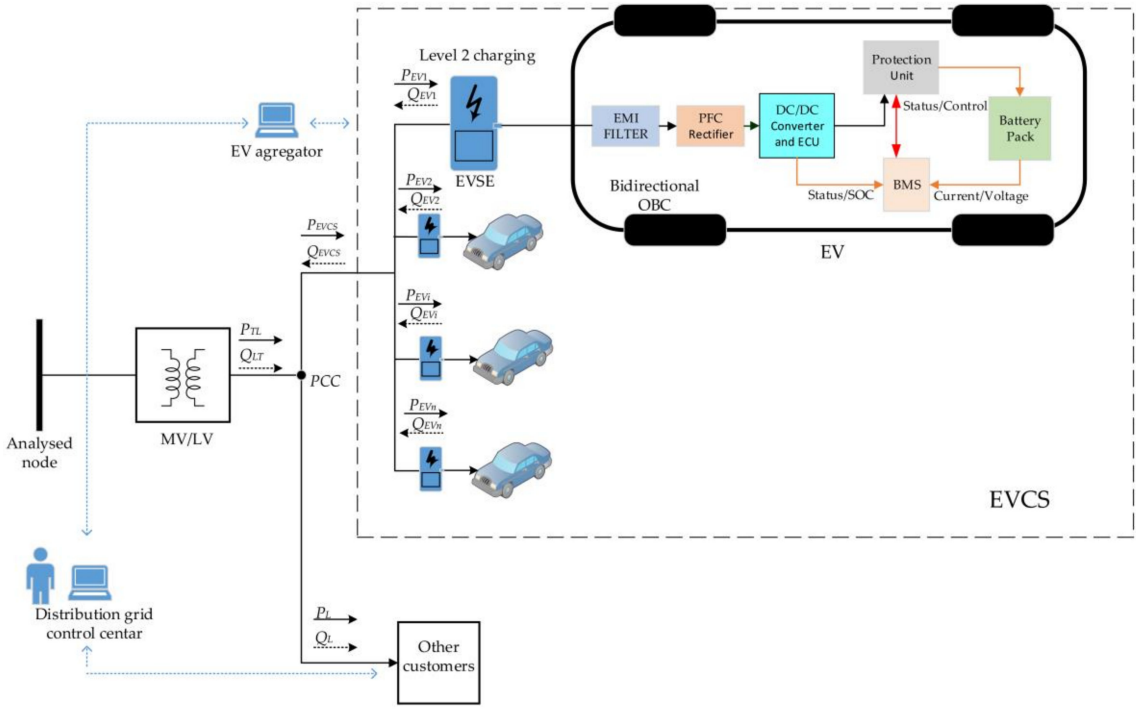

Figure 3. Proposed reactive power support diagram using OBC from EVCS.

2.2.2. Mobility Stochastic Behavior Model

There is a large number of papers dealing with the optimal structure of EVCSs, which refers to number of charging spots, types of charging and technology of chargers themselves [53–55]. In this paper, the charging demand of EVCSs is obtained using the number of EVs that arrive at the EVCS during 24 h as an input. Furthermore, the random nature of EV arrival time, electrical efficiency, battery capacity and daily miles driven are respected in order to obtain EVCS demand. In this paper, the stochastic nature of EV load is modeled using probability density functions (PDF) for two parameters: plug-in time and miles traveled before last charge.

- Behavior of start charging time

A PDF of vehicles' arrival time is obtained from [56], where the results of a large number of measurements from public charging stations have been analyzed. Based on actual data, the multimodality of distribution has been described using the Beta Mixture Model (BMM), which has proved to be appropriate for analysing EV data, [56].

A corresponding density function from the BMM model is obtained by summing up the beta distributions of different parameters and weight factors. The beta distribution of probability density is defined by the following equation:

$$\text{Beta}(x \mid a, b) = \frac{\Gamma(a+b)}{\Gamma(a)\Gamma(b)} x^{a-1} x^{b-1}, \quad (1)$$

where $\Gamma(.)$ is gamma function, a and b are parameters which define the shape of distribution and x is a parameter from the interval between [0, 1].

The BMM is represented by the following sum:

$$\text{BMM}(x) = \sum_{m=1}^{M} (w_n \text{Beta}(x \mid a_m, b_m)) \quad (2)$$

wherein the sum of weights are equal to one:

$$\sum_{m=1}^{M} w_n = 1 \quad (3)$$

Obtained PDFs for working days and weekends plug in times are presented in Figure 4, while parameters of BMM are given in Table 2. The values in Table 2 are rounded to two decimal places [56].

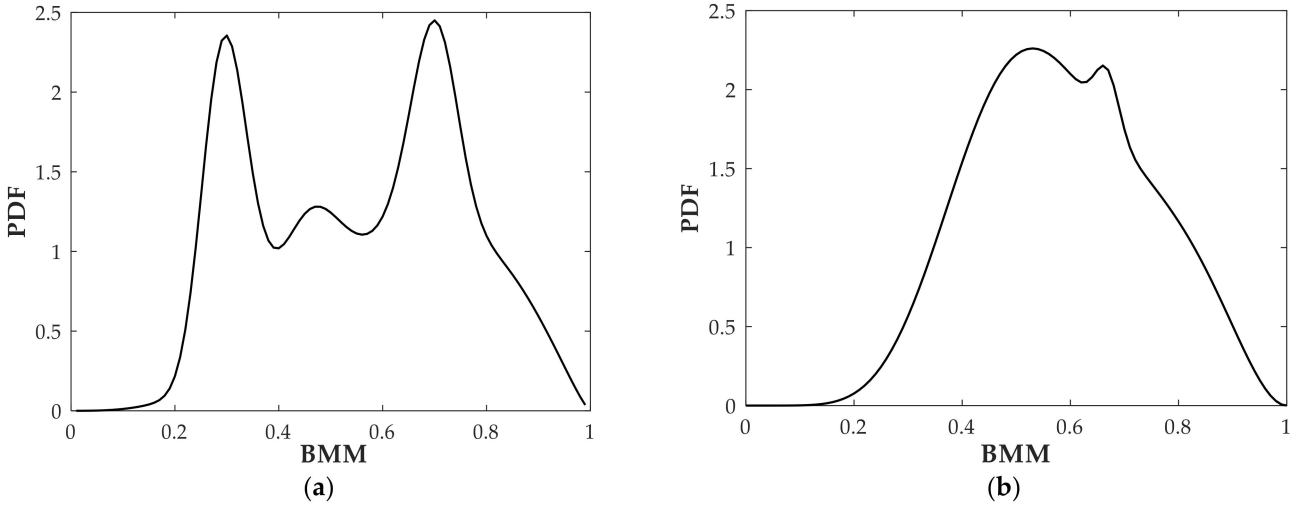

Figure 4. PDF for plug in time for: (**a**) Working day; (**b**) Weekend.

Table 2. Parameters for BMM model.

Bus Type	Working Day	Weekend
Number of modes	4	3
Parameter a	32.80 76.42 4.13 36.12	300.71 8.69 6.22
Parameter b	76.76 33.40 2.34 42.65	150.08 9.12 3.05
Weights	0.23 0.14 0.56 0.08	0.02 0.48 0.50

- Behavior of distance travelled and initial state of charge

In order to determine the energy required to charge vehicles, it is necessary to predict the level of the charge of a battery (SOC) of a single EV. An important factor for this is to determine daily miles traveled. The lognormal distribution of the distance travelled function has been shown to be suitable for describing the mileage distribution functions, and is represented by way of [6]:

$$g(d,\mu,\sigma) = \frac{1}{d\cdot\sqrt{2\pi\sigma^2}} e^{-\frac{(\ln d-\mu)^2}{2\sigma^2}},\ d>0 \tag{4}$$

The distribution parameters depend on a driver's habits in the area being analyzed. Statistics on the conventional vehicles are often taken into account due to insufficient data of EVs. This paper uses statistical data that 50% of drivers drive less than 25 miles during the day, and 80% of drivers travel less than 40 miles [57]. The corresponding lognormal distribution of daily traveled miles and coresponding CDF are presented at Figures 5 and 6, with mean value μ = 3.37 and standard deviation σ = 0.5 [58].

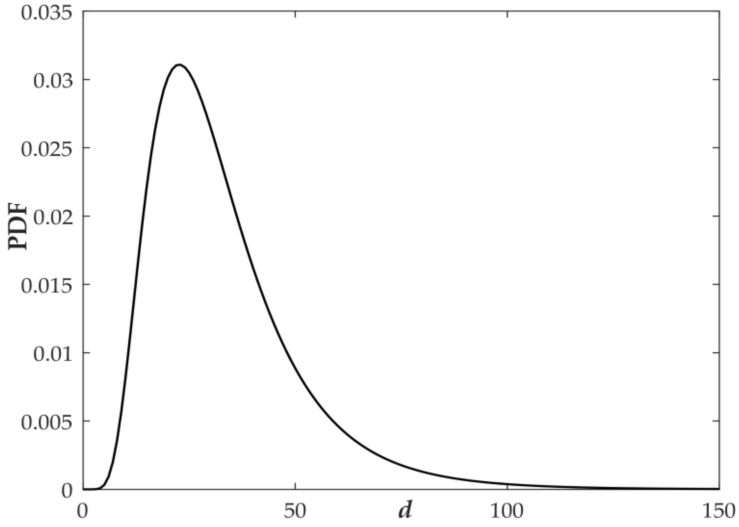

Figure 5. PDF of daily distance traveled of EV.

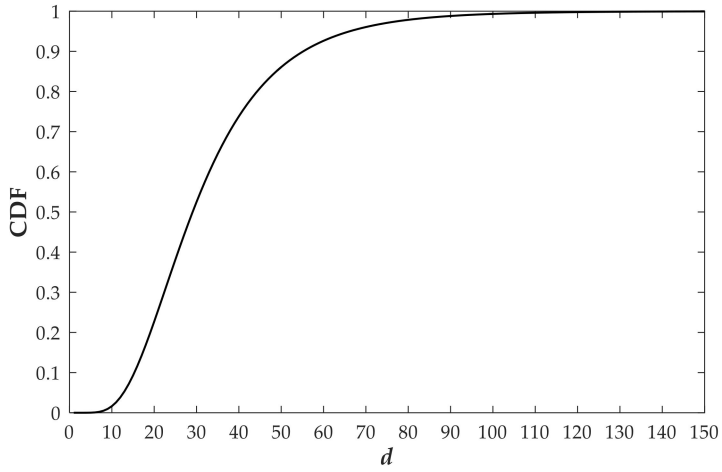

Figure 6. CDF of daily distance traveled of an EV.

Now, the initial state of the charge can be determined as shown below [6]:

$$SOC_i(x) = \left(1 - \frac{E_{cons} \cdot d}{C_b}\right) \cdot 100 \quad (5)$$

where C_b battery capacity in kWh, E_{cons} is energy consumtion in kWh per miles and d estimated daily distance traveled in miles.

2.2.3. Charging Power Model

Considering the latest statistics of dominating shares of EV types, [59,60] all EVs charged in this study have 71% probability of being a battery electric vehicle (BEV) and 29% probability of being a plug-in hybrid electric vehicle (PHEVs).

Electric car economy changes all the time, depending on things such as road gradient and car speed. In this paper, electrical efficiency and battery capacity are taken as random numbers between values given in Table 3 depending on the type of EV.

Table 3. Parameters of BMM model.

EV Types	BEV	PHEV
Number of vehicles [%]	71	29
Battery capacity [kWh]	40–80	10–16
Electrical efficiency [kWh/mile]	0.25–0.40	0.25–0.40

In order to sustain a longevity, it is known that whole battery's energy capacity is usually not fully utilized. It has been found that between 78–95% of the full batteries capacity is used for different EV models [60]. The required value of SOC_{req} for the user is taken to be 95% [6,61,62]:

$$E_{req} = \frac{(SOC_{req} - SOC_i) \cdot C_b}{\eta \cdot 100} \quad (6)$$

where η is charging efficiency 0.95. The duration of EV charging depends on the required energy and charging power of EV and is equal to:

$$T_{ch} = \frac{E_{req}}{P_{EV}}, P_{EV} = \begin{cases} 3.4\text{kW, PHEV} \\ 7.2\text{kW, BEV} \end{cases} \quad (7)$$

2.3. Power Flow Analysis

Power flow or load flow calculations are very fundamental for all power system analyses. It is a very important tool for power systems planning, design, operations, maintenance, optimization and control. At the planing stage, load flow analysis is used to determine: the location of distributed generators, the location of capacitors, economic scheduling, power quality improvements, network reconfiguration, power systems optimization and other applications. Furthermore, in order to plan future growing load demands, power flow analysis is necessary. At the operation stage, it is run to explore system stability and to improve efficiency. Usage of power flow analysis enables that maintenance plans can proceed, without violating power system security. Load flow studies are performed for the determination of the steady state operating condition of a power system. Input parameters of power flow analysis of distribution network are network topology and network parameters, as well as load and generator models. Power flow calculations are performed by iterative methods. The most common power flow calculation methods are Gauss–Seidel Method, Newton–Raphson Method and Fast Decoupled Method. These methods are not appropriate for distribution systems due to their special characteristics such as low line X/R ratios, unbalanced load, radial or weakly meshed network structure and large number of nodes, etc. These features make distribution systems power flow computation different to analyze, as compared to the transmission systems. There is a number of methods proposed in the literature for the solution of power flow problem in radial distribution networks [63]. Back–forward sweeping (BFS) iterative method is suitable for calculations of radial distribution system load flow, which is analyzed in this paper [64]. The algorithm is very robust and numerically efficient for convergence. It is applicable for a wide variation of distribution networks. The algorithm begins with an initial solution for all node voltages and performs basic steps until a convergence criterion is satisfied. In the backward step, currents of each branch are calculated. Bus voltages are updated in a forward sweep starting from the first branch and moving towards end branches. After the convergence criterion has been satisfied, node voltages, currents in branches and active and reactive power losses are determined. This iterative method is implemented in Matlab for calculating power losses in radial IEEE 33 bus network. Different load types together with EVCS demands are implemented in this model. In this paper, power flow analysis has been used from the planning aspect, as a part of the optimization process for determinating optimal positions for EVCSs in an analyzed network. Additionally, it is used for calculating power losses for different EVCS demands level.

3. Methodology

3.1. Description

A flowchart of the proposed methodology is shown in Figure 7. The methodology includes both global and local solution approaches. The global one refers to the modeling and analysis of the power network and the determination of active power losses in the network, and the local one to the determination of the aging of the selected distribution transformer. The proposed algorithm consists of four steps. In the first step, network data and nodal loads are entered. Additionally, active and reactive nodal power are defined depending on a type of load (industrial, commercial or residential) according to Figure 1. Then, in this step, the number of stations are entered, as well as the data needed to determine the EVCS demand. The stochastic nature of EV charging is taken into account and explained in detail in Section 2. The second step of the proposed methodology includes the position of EVCSs in the power system. More precisely, in this step, a matrix that includes the possible positions of EVCSs is formed. In this step, the criterion that only one station can be placed in each part of the network has been met. The proposed methodology takes into account the fact that it is possible to divide the network into an arbitrary number of parts, and in each part of the network an arbitrary number of stations can be found. The third step represents the calculation of the electrical parameters of the network. In this step, the method for calculating power flows according to the characteristics of the network is implemented. In the fourth step, the locations of EVCSs are selected based on the criterion of minimum network losses, defined by the following equation:

$$J = \min P_l = \sum_{i=1}^{B} P_{li} \tag{8}$$

where i, B, P_l and P_{li}, are the index, total number of branches, total active power and active power losses of branch i, respectively.

In this paper, optimization is achieved by searching the obtained results, so that the focus of paper is not the development and improvement of optimization methods. Nevertheless, it is important to note that in the last few years, different methods have been developed and applied to account for optimal power flows in the energy system or for different types of examples that comply with different limitations. Some of them are detailed and tested in papers [65–68]. In the fifth step, the final value of reactive power injection of the EVCSs is selected. Namely, in this step, by choosing the final value of the reactive power injected by EVCSs, the influence of the reactive power on the losses of active energy and on transformer aging through which the station is connected to the grid is affected. In this paper, the GRA method is used for determining the final value of reactive power.

After obtaining the best positions for EVCSs, off-grid managing of the EVCSs has been proposed. Based on the predicted daily diagram of EVCSs and other consumption, the station operator evaluates the optimal daily reactive power injection from EVs, i.e., power factor of on-board chargers of EVs in EVCSs. The proposed methodology assume that power factor of OBC is constant during the 24 h period. Detailed post-optimization analysis of the reactive power injection from EVs at EVCSs to energy losses and transformer aging has been performed.

It is important to emphasize that the performed post-optimization analysis represents an incremental contribution in relation to the paper [15], since it is extended to include transformer aging analyzis. Based on the performed analyses, the correlation of the impact of reactive power on energy losses and the impact of reactive power on transformer aging can be clearly seen.

The aim of this paper is to explore the possibility of the impact of reactive power from oversized OBCs on active power losses and on transformer aging. With regard to experimental confirmation of the obtained results, at this stage it was primarily necessary to computerize a model and verify the simultaneous influence of active energy losses and

transformer aging. On the other hand, the impact of chargers on losses in the distribution system in real-time circumstances is very difficult. Furthermore, one of the bigger obstacles so far is the number of EVs, because in whole of Montenegro there are only 126 EVs [69] and these are vehicles that have chargers that are not pre-dimensional. Relatively small oversizing of the OBCs is the basis of the assumption of this paper.

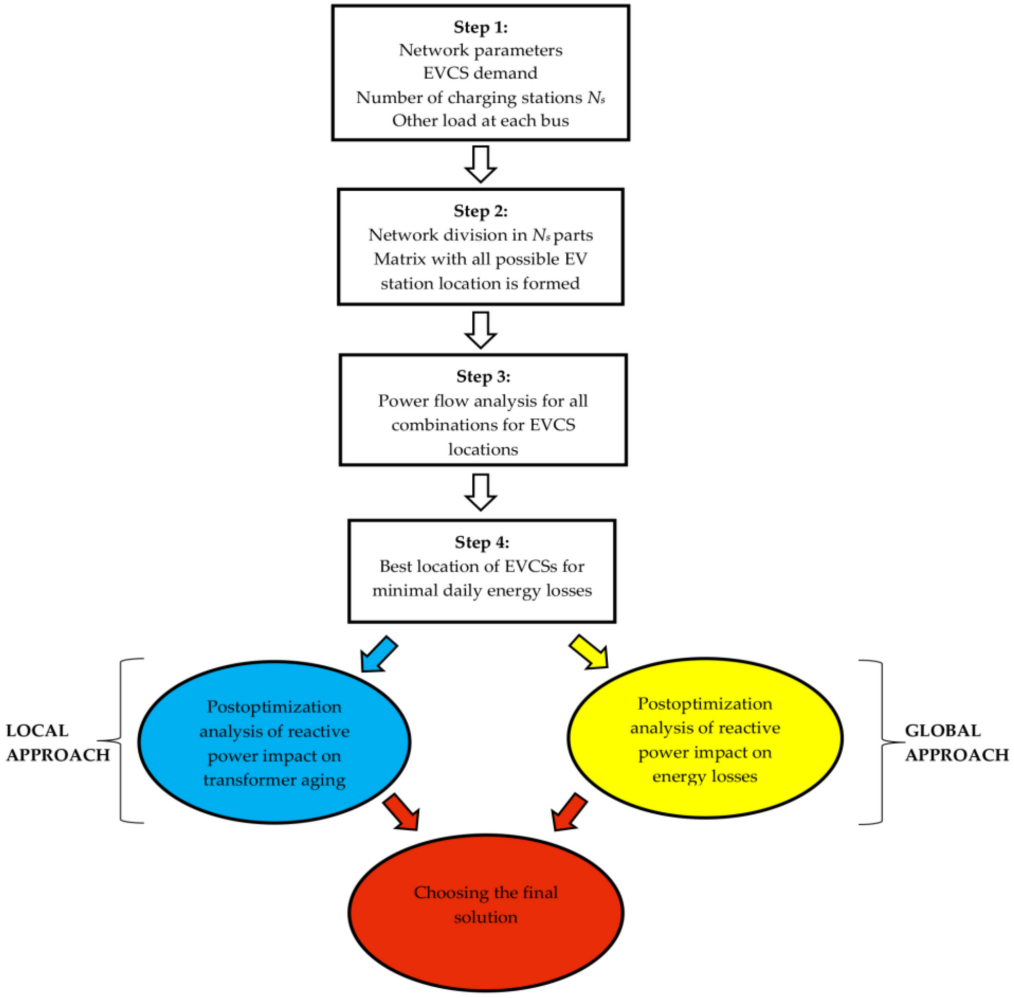

Figure 7. Flowchart of proposed methodology.

3.2. Sample Generation with Monte Carlo

The Monte Carlo (MC) statistical method was used to obtain the daily EVCS demand. The method requires that parameteres of the physical system, in this case EVCS demand, are described as PDFs.

When these functions are known, the MC simulation continues with a random selection of values from functions. For this purpose, the inverse transformation method was used, which states that any probability distribution can be obtained from a uniform probability distribution, if an inverse cumulative probability distribution can be determined [70]. A flowchart of the generation of a EVCS demand profile is given in Figure 8.

To terminate the MC process criteria number of MC iterations is used. The process was set to repeat until reaching 5000 iterations.

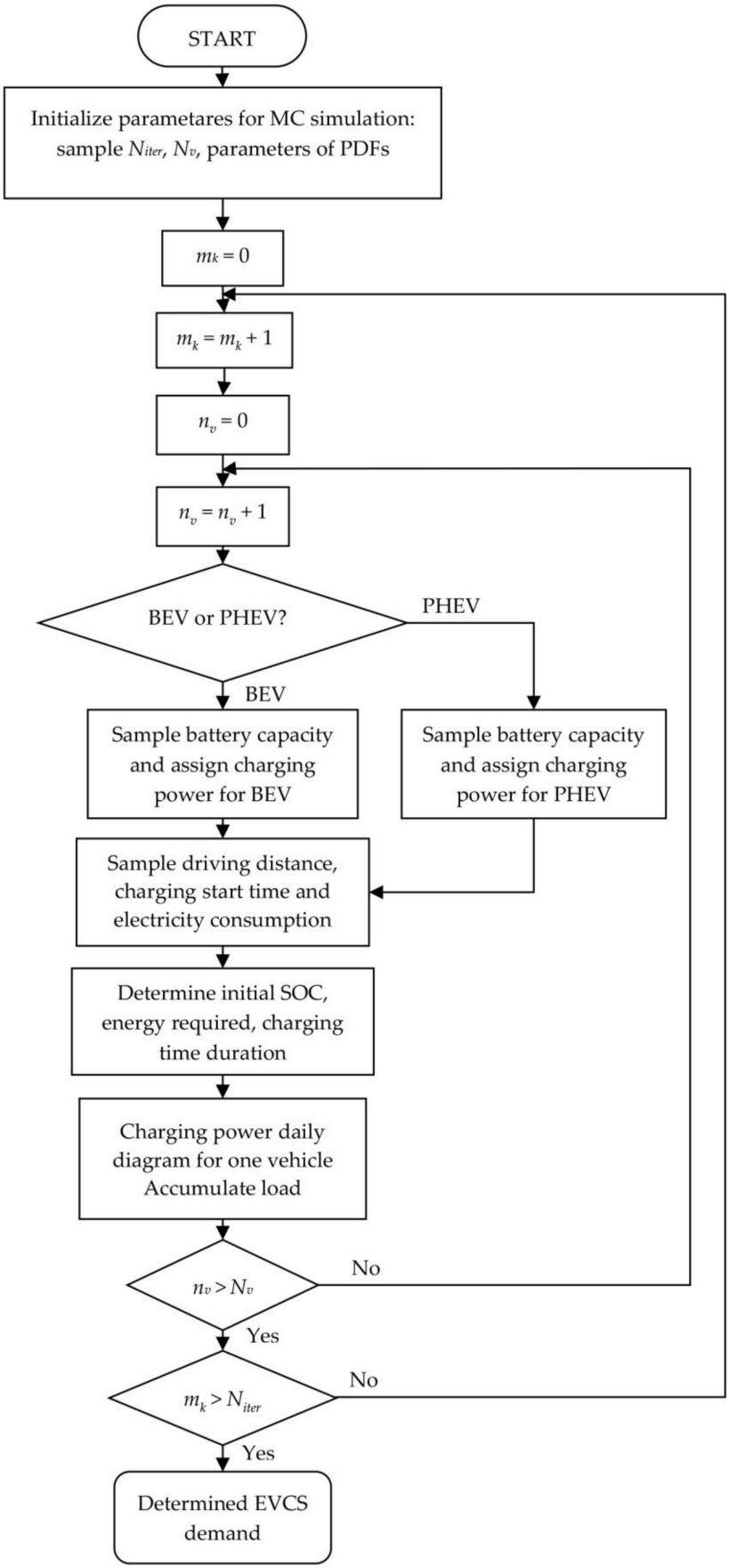

Figure 8. Flowchart for EVCS demand.

3.3. Transformer Aging Model

The insulation system of mineral oil transformers is composed of thermally upgraded oil-impregnated paper. Cellulose deterioration is influenced by hydrolysis, oxidation and pyrolysis which are the consequences of water, oxygen and heat, respectively. Taking into consideration that exposure to moisture and oxygen in transformers are generally reduced, the most significant determining factor to insulation deterioration is the heat. Transformer heating is caused primarily by energy losses. The majority of losses are located in magnetic core (no-load losses) and the windings (load losses). No-load are hysteresis and eddy current losses, while winding losses are primarily due to DC losses and stray load loss due to the eddy currents induced in other structural parts of the transformer. All these losses cause heating in the corresponding parts of the transformer. The most critical part for the transformer isolation system is placed where temperature has maximum value, which is known as hot spot temperature [4].

According to the loading guides, IEEE guide for loading mineral-oil-immersed transformers [37], the hot-spot temperature in a transformer winding consists of three components:

$$\theta_H = \theta_A + \Delta\theta_{TO} + \Delta\theta_H \tag{9}$$

where θ_H, is the winding hottest-spot temperature, °C, θ_A, is the average ambient temperature during the load cycle to be studied, °C, $\Delta\theta_{TO}$ is the top-oil rise over ambient temperature, °C, and $\Delta\theta_H$ is the winding hottest-spot rise over top-oil temperature, °C.

As is proposed in the IEEE guide, θ_A is constant and equals to 30 °C. The top-oil rise over ambient temperature is given in the following equation:

$$\Delta\theta_{TO} = (\Delta\theta_{TO,u} - \Delta\theta_{TO,i}) \cdot \left(1 - e^{-t/\tau_{TO}}\right) + \Delta\theta_{TO,i} \tag{10}$$

where τ_{TO} top-oil time is constant, $\Delta\theta_{TO,i}$ and $\Delta\theta_{TO,u}$ are the initial and ultimate top-oil rises over ambient temperature, respectively, which equals to:

$$\Delta\theta_{TO,i} = \Delta\theta_{TO,R} \cdot \left[\frac{(K_i^2 \cdot R + 1)}{R + 1}\right]^n \tag{11}$$

$$\Delta\theta_{TO,u} = \Delta\theta_{TO,R} \cdot \left[\frac{(K_u^2 \cdot R + 1)}{R + 1}\right]^n \tag{12}$$

In the previous equations, $\Delta\theta_{TO,R}$ is the top-oil temperature rise over ambient temperature at rated load, k_i and k_u represent the ratio of initial and ultimate load to rated load, per unit, n is an empirically derived exponent which depends on a cooling mode and describes effects of change in oil resistance to change in load, while R is the ratio of a load loss at a rated load to a no-load loss. The top-oil time constant at a rated kVA is given in the following equation. The time constant equals to:

$$\tau_{TO} = \tau_{TO,R} \frac{\left(\frac{\Delta\theta_{TO,u}}{\Delta\theta_{TO,r}}\right) - \left(\frac{\Delta\theta_{TO,i}}{\Delta\theta_{TO,r}}\right)}{\left(\frac{\Delta\theta_{TO,u}}{\Delta\theta_{TO,r}}\right)^{\frac{1}{n}} - \left(\frac{\Delta\theta_{TO,i}}{\Delta\theta_{TO,r}}\right)^{\frac{1}{n}}} \tag{13}$$

Transient winding hottest-spot temperature rise over top-oil temperature is equal to:

$$\Delta\theta_H = (\Delta\theta_{H,u} - \Delta\theta_{H,i}) \cdot \left(1 - e^{-t/\tau_w}\right) + \Delta\theta_{H,i} \tag{14}$$

In Equation (14), $\Delta\theta_{H,i}$ and $\Delta\theta_{H,u}$ represent the initial and ultimate winding hottest-spot rises over top-oil temperature in °C, which equals to:

$$\Delta\theta_{H,i} = \Delta\theta_{H,R} \cdot K_i^{2m} \tag{15}$$

$$\Delta\theta_{H,u} = \Delta\theta_{H,R} \cdot K_u^{2m} \tag{16}$$

where $\Delta\theta_{H,R}$ is the winding hottest-spot rise over top-oil temperature at rated load. Parameter m describes changes in resistance and oil viscosity with changes in load.

Calculating the temperature of the hottest spot allows the determination of important parameters that describe transformers' aging, which are the accelerated transformer aging factor F_{AA} and LOL.

The aging acceleration factor for a given load and hottest spot temperature can be obtained as shown in Equation (17):

$$F_{AA} = e^{\left[\frac{15000}{383} - \frac{15000}{\theta_H + 273}\right]} \tag{17}$$

If $F_{AA} > 1$, the transformer is experiencing accelerated aging. According to [37], normal aging occurs at the reference hottest-spot temperature of 110 °C, where $F_{AA} = 1$. The equivalent aging factor F_{EQA} is further obtained as indicated below:

$$F_{EQA} = \frac{\sum_{j=1}^{N} F_{AA,j} \Delta t_j}{\sum_{n=j}^{N} \Delta t_j} \tag{18}$$

where j is the time intervals index, N is the total number of time intervals, Δt is the time interval, $F_{AA,j}$ is the aging acceleration factor for j-th time interval. The percentage of shortening the isolation life of a transformer is calculated as shown in the relation below:

$$\%LOL = \frac{F_{EQA} \cdot t \cdot 100}{\text{Normal insulation life}} \tag{19}$$

The value of the normal duration of insulation, [37], is taken to be 18,000 h or 20.55 years. Therefore, when the temperature of the hottest point is 110 °C for 24 h, the percentage of the daily shortening of the lifespan is equal to:

$$\%LOL = \frac{24 \cdot 100}{180,000} = 0.01333\% \tag{20}$$

3.4. Transformer Loading with EVCS

Adding EVCS demand at node n to the distribution transformer affects its loading, and therefore can cause further transformer aging. The available reactive power of inverters of EVs can be utilized for reactive power compensation in order to improve power loss reduction and prevent transformer aging. The total active load of the transformer at node k, P_{TL_k}, is equal to:

$$P_{TL_k} = P_{L_k} + P_{EVCS_k} \tag{21}$$

where P_{L_k} and P_{EVCS_k} re the sum of load without EVs and active power demand of EVCSs at node k. In case, during the charging of EVs, reactive power is injected, the total reactive load of transformer Q_{TL_n} is equal to:

$$Q_{TL_k} = Q_{L_k} - Q_{EVCS_k} \tag{22}$$

where Q_{L_k} represents the sum of the load without EVs and Q_{EVCS_i} is reactive power injected from EVCSs obtained from EV charging inverters at node k. Injecting reactive power to the transformer at node k has an influence on reducing the apparent power of the total load and therefore the loading and temperature of the transformer as well.

3.5. Grey Relational Analysis (GRA)

The selection of the final solution is done using Grey Relational Analysis (GRA). The GRA is a multiple-attribute decision-making method and it is widely applied in electric power systems [71–74]. GRA is performed in several steps. In the first step, n alternatives

sequences with m criteria are formed. Y_i represents i-th alternative sequence, and value y_{ij} represents the value of attributes j of alternative i:

$$Y_i = \left(y_{i1}, y_{i2}, \ldots y_{ij}, \ldots, y_{in}\right) \tag{23}$$

The second step of the GRA procedure is normalization, which converts the data to values between [0,1]. The smaller the normalization used in this case, the better, since smaller values are prefered in the problem desribed in this paper. The comparability sequence is as follows:

$$X_i = \left(x_{i1}, x_{i2}, \ldots x_{ij}, \ldots, x_{in}\right) \tag{24}$$

is obtain using the equation below:

$$x_{ij} = \frac{max\left\{y_{ij,} i = 1, 2, \ldots, m\right\} - y_{ij,}}{max\left\{y_{ij,} i = 1, 2, \ldots, m\right\} - min\left\{y_{ij,} i = 1, 2, \ldots, m\right\}} \tag{25}$$

where i = 1, 2, . . . , m, and j = 1, 2, . . . , n.

Reference sequence X_0 is defined as (x_{01}, x_{01}, . . . , x_{01}, . . . x_{01}) = (1, 1, . . . , 1, . . . 1). The aim is to find an alternative whose comparability sequence is closest to the reference sequence. For this purpose, the Grey Relational Coefficient (GRC) between x_{ij} and x_{0j}, is calculated using the equation:

$$\gamma\left(x_{0j}, x_{ij}\right) = \frac{\Delta_{min} + \xi \cdot \Delta_{max}}{\Delta_{ij} + \xi \cdot \Delta_{max}} \tag{26}$$

where i = 1, 2, . . . , m, and j = 1, 2, . . . , n.

The values of Δ_{ij}, Δ_{min}, Δ_{max}, ξ, are defined as:

$$\Delta_{ij} = \left| x_{0j} - x_{ij} \right| \tag{27}$$

$$\Delta_{min} = Min\left\{\Delta_{ij},\ i = 1, 2, \ldots, m; j = 1, 2, \ldots n\right\}, \tag{28}$$

$$\Delta_{max} = Max\left\{\Delta_{ij},\ i = 1, 2, \ldots, m; j = 1, 2, \ldots n\right\}, \tag{29}$$

$$\xi \epsilon [0, 1] \tag{30}$$

For this purpose, 0.5 is usually used as the distinguishing coefficient value ξ.

For the problem described in this paper, the total number of alternatives which are compared equals the number of optimal solutions obtained from Pareto, while the elements of the sequence are the values of two criteria: transformer daily aging and active power losses. Now, in order to determine the best solution, it is necessary to determine the Grey Relation Grade (GRG). GRG is calculated by using the following equation:

$$\Gamma(X_0, X_i) = \sum_{j=1}^{n} w_j \cdot \gamma\left(x_{oj}, x_{ij}\right) \tag{31}$$

where w_j represents the weight factor for the corresponding index. The alternative with the highest GRG would be the best choice.

4. Analysis and Results

For the purpose of the analysis, the IEEE medium voltage radial distribution network with 33 bus has been modeled, Figure 9. The base voltage of the network is 12.66 kV, and the base power is 100 MVA. Line parameters are taken from [75]. Daily active power demand, without public stations, is 62,556 kWh. Total daily active energy losses, obtained from the power flow analysis amount to 2924 kWh. The lowest value of voltage in the system occurs during the 18th hour at bus 18 with the value of 0.9016 p.u.

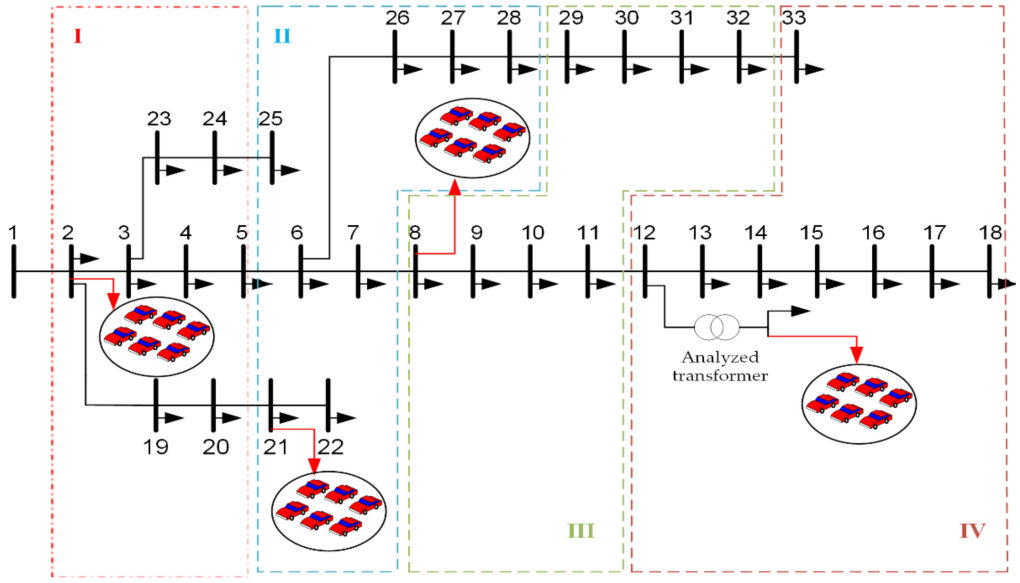

Figure 9. Single-line diagram of 33-bus test system.

4.1. EVCSs Location Impact of Active Energy Losses

The proposed methodology, Figure 7, enables us to perform an analysis of the impact of EVs on losses for an arbitrary number of EVCSs. In this paper, it is adopted that it is necessary to build four EVCSs. Based on the calculation of power flow, the best and worst cases in terms of energy losses are determined by the "brute force" algorithm. The results of the power flow calculations and algorithm are shown in Table 4 below. OBCs of EVs are assumed to operate with a unit power factor.

Table 4. Best and worst cases for EVCSs locations.

Parameters	Without PEV Load	With Public Charging Stations	
		Best Case	Worst Case
Location of charging station	-	2, 19, 20, 21	15, 16, 17, 18
Daily active power demand [kWh]	62,557	72,152	72,152
Daily active energy loss [kWh]	2924	3008	4486
Lowest voltage value in p.u.	0.9016 (18 h, bus 18)	0.9012 (18 h, bus 18)	0.8422 (18 h, bus 18)

Table 4 shows a comparison between the parameters with or without charging stations and a comparison between the best and worst cases for charging station positions when energy losses are concerned.

There is a clear difference in losses depending on the location of EVCSs. In the best case, the increase in daily losses is 3% and in the worst case, it is 53% compared to the case without charging stations. These results show a significant influence of location of charging stations on network losses.

4.2. Impact of Reactive Power from EVCSs on Energy Losses

From the previously obtained results shown in Table 4, it can be seen that the obtained locations of EVCSs are in a row, so it can be assumed that they will not satisfy the needs of EVs that are far from such station. For this purpose, the spatial division of the network into four parts is proposed, so that each separate part includes eight nodes, see Figure 9 [76].

The proposed methodology, Figure 7, also allows an arbitrary division of the network with an arbitrary number of nodes.

After the division of the network, it is necessary to determine one location in each zone of the network where a station for electric vehicles would be placed. In this part of

the paper, the impact of the power factor of on-board chargers on active energy losses is analyzed.

Accordingly, two scenarios are considered: the first scenario is that EVs are charged with a unit power factor; the second scenario is that vehicles are charged with the same active power as in the first case, and the maximum reactive power capacity from on-board chargers is used. As is mentioned in Section 2, it is assumed that on-board charges are oversized by 5.3%. The results are summarized in Table 5 below.

Table 5. Locations for EVCSs and network parameters for the two scenarios.

Parameter	Scenario 1 No Reactive Power Support	Scenario 2 Reactive Power Support
Location of charging station	2, 21, 8, 12	2, 21, 8, 12
Daily active energy loss [kWh]	3419.34	3320.00
Lowest voltage value in p.u	0.8889	0.8920
(time and number of bus)	(18 h, bus 18)	(18 h, bus 18)

As can be seen in Table 5, for analyses of the nework and proposed network division, reactive power injection from on-board chargers does not have influence on EVCSs location. On the other hand, reactive power injection has an influence on daily acitive energy losess. Namely, it is shown that with a relatively small oversizing of the inverter, it is possible to reduce the loss of active power by about 3% without any interruption of an EV driver's habits or charging behavior.

Bearing in mind that voltage level of 12.33 kV, at which the R/X ratio is not large, produces the expected results obtained by these voltages. More precisely, the lowest voltage in the network in case the stations provide reactive power, is slightly higher compared to the scenario where the stations' power factor is 1.

4.3. Impact of Reactive Power from EVCS on Transformer Aging

The effect of reactive power injection on transformer aging is shown in Tables 6 and 7 below. The percentages in the tables refers to the gradual increase in power of EVCSs in relation to higher EV penetration. The results were obtained based on the formulas from Section 3.2. Two standardized distribution transformers 11/0.433 kV of different rated power, T_1 (200 kVA) and T_2 (250 kVA) have been compared in order to determine the appropriate power transformer for the analysed bus 12. Thermal parameters of transformers are taken from [33].

Table 6. LOL for different levels of reactive power for T_1 for different additional penetration level.

Q/Q_{max}	Working Day EV Additional Penetration [%]					Weekend EV Additional Penetration [%]				
	0	4	7	10	20	0	4	7	10	20
	LOL %					LOL %				
1	0.0082	0.0129	0.0183	0.0260	0.0831	0.0065	0.0102	0.0142	0.0198	0.0613
2/3	0.0076	0.0119	0.0168	0.0235	0.0728	0.0061	0.0094	0.0130	0.0180	0.0537
1/3	0.0080	0.0124	0.0174	0.0242	0.0740	0.0063	0.0097	0.0133	0.0184	0.0540
1/5	0.0084	0.0131	0.0182	0.0253	0.0771	0.0066	0.0102	0.0139	0.0192	0.0563
0	0.0094	0.0145	0.0202	0.0282	0.0856	0.0074	0.0112	0.0155	0.0213	0.0623

Table 7. LOL for different levels of reactive power for the T_2 for different additional penetration levels.

Q/Q_{max}	Working Day EV Additional Penetration [%]					Weekend EV Additional Penetration [%]				
	0	**20**	**40**	**50**	**60**	**0**	**20**	**40**	**50**	**60**
	LOL %					**LOL %**				
1	0	0.0024	0.0148	0.0379	0.0977	0	0.0020	0.0118	0.0294	0.0729
2/3	0	0.0021	0.0127	0.0316	0.0787	0	0.0018	0.0101	0.0244	0.0591
1/3	0	0.0022	0.0124	0.0305	0.0749	0	0.0018	0.0099	0.0234	0.0559
1/5	0	0.0022	0.0128	0.0313	0.0768	0	0.0019	0.0102	0.0241	0.0572
0	0	0.0024	0.0139	0.0341	0.0835	0	0.0020	0.0110	0.0261	0.0620

There is a large number of papers the optimal transformer sizing [77] and especially transformer sizing with the presence of electric vehicle charging [78]. In this paper, we only take these to values for rated power for purpose of analysis based on the overall load which is sum of EVCS load and the other load for the analysed bus 12.

In Table 6, LOL percentage for a workday and weekend are represented for different values of reactive power injection during the EV charging for T_1.

Since the daily energy consumption from EVCS during the weekend, and mainly concentrated in the central part of the day, is about 18% lower than during the weekday [56], the values for LOL are expected to be lower than during the weekday.

From Table 6, it can be concluded that different values of reactive power injection by the chargers also have different values of LOL. Namely, on the basis of Table 6, it is shown that, with an increased penetration of 4% per working day, LOL values change between 0.0129% and 0.0145 %. From Equation (20), it can be concluded that if the LOL value is greater than 0.01333%, additional aging of the transformer occurs. As we can see, with increased penetration of 4% per working day, with some injection level of reactive power, there is no additional aging. If reactive power injection is zero, than LOL = 0.0145% which means (0.0148 × 180,000/100 = 26.1 h) 26.1 h over the 24 h period. That means 2.1 h of additional ageing every day. It can also be noted that for values of reactive power $Q = 2/3Q_{max}$, LOL has a minimum value for each considered level of EV penetration. Within this case, with a higher degree level of reactive power, LOL is reduced compared to the case when there is no injection of reactive power from the vehicle charger. For this case, in Figure 10, the reactive load of the transformer per hour without reactive power from the vehicle (in blue color) is shown, and the reactive load of the transformer with the reactive power injection from EVs (in yellow) is shown as well. As it can be seen, there is a compensation of reactive power in the largest portion of the day. This has resulted in reduced apparent power for almost the entire duration of the day, Figure 10.

There is similar situation with the increase of 7% for the weekend, with adequate reactive power support there will be no aging during the weekend. If there is no reactive power support there will be 27.9 h daily aging over the 24 h period. That means 3.9 h of additional ageing every day.

As is presented in Table 6 for the example of the EV penetration increase of 7% at a EVCS, the daily aging value is 36.6 h (for $\cos\varphi = 1$) to 30.24 h (for $Q = 2/3Q_{max}$) representing a decrease of 17.37%. During the working day with 7% additional EV penetration, daily transformer LOL reaches 0.0202%. With reactive power injection of $2/3Q_{max}$, there is a decrease of daily aging from 36.36 h to 30.24 h, which is a 17% decrease. Even though it is significant reduction, hot spot temperature reaches 140 °C, which represents a critical value at which gas bubbles appear [35].

From Table 7, it can be seen that transformer T_2 with an increased penetration of 40% increases aging on the working day with 25 h aging over the 24 h period with no reactive power support. What is interesting is that LOL is higher at maximum reactive power support compared to where $\cos\varphi = 1$ and it is 26.64 h.

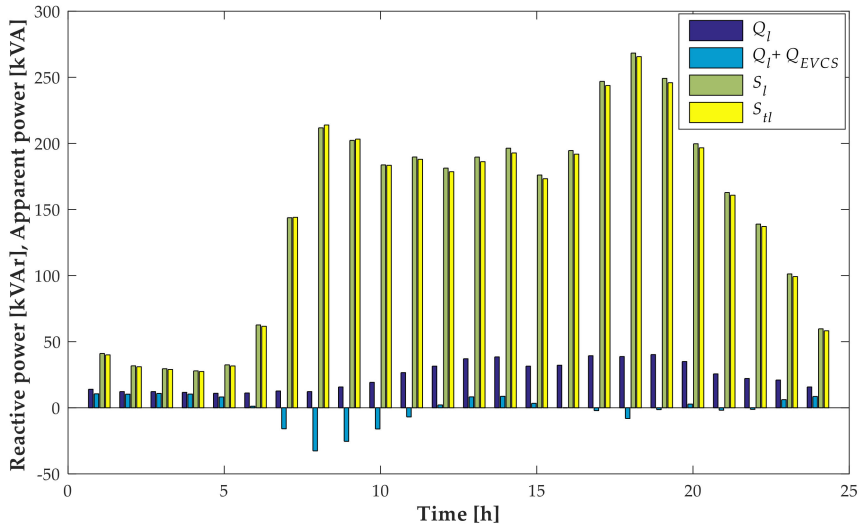

Figure 10. Reactive and apparent power loading of T_1 with (S_{tl}) and without reactive power (Q_{EVCS}) from EVCSs (S_l), with 4% increase in EVCS demand.

As is shown in Table 7, with an adequate value of reactive power, the value of LOL is less than 0.0133%. Furthermore, as in the previous case, there is an improvement in decreasing the aging, using reactive power from EVs. The change in daily aging of the transformer and daily energy losses in the function of reactive power injection are presented in Figures 11 and 12, for transformer T_2 with EV adiditional penetration of 40%. From the obtained characteristics, it can be seen that for some power injection there is aditional aging (above 24 h). So, it can be concluded that there is an optimal value of reactive power support that can have a positive influence on both transformer aging and energy losses.

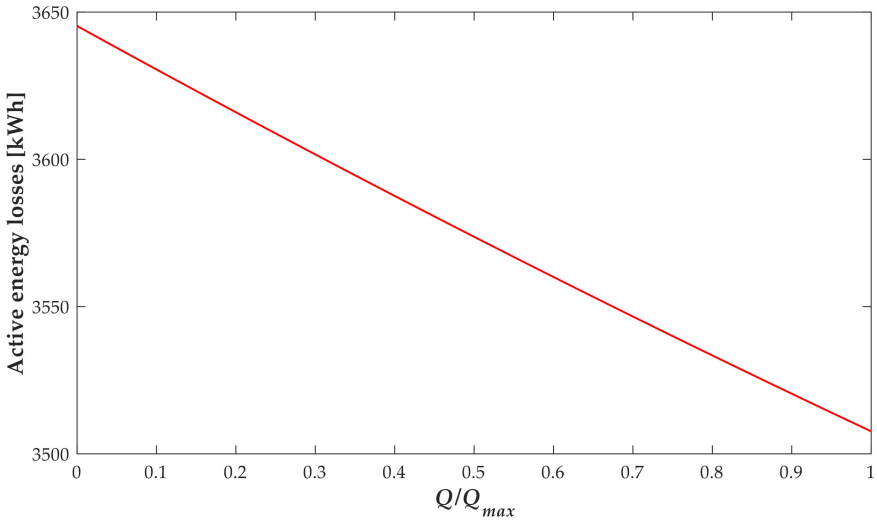

Figure 11. Change in active daily losses in function of reactive power from public EVCSs.

In order to better understand the mutual influence of reactive power on transformer aging and active energy losses, solutions that satisfy the Pareto principle of non-dominance are shown in Figure 13. The presented solutions have been obtained by changing the reactive power range from 0 to Q_{max} with a step of $0.05Q_{max}$.

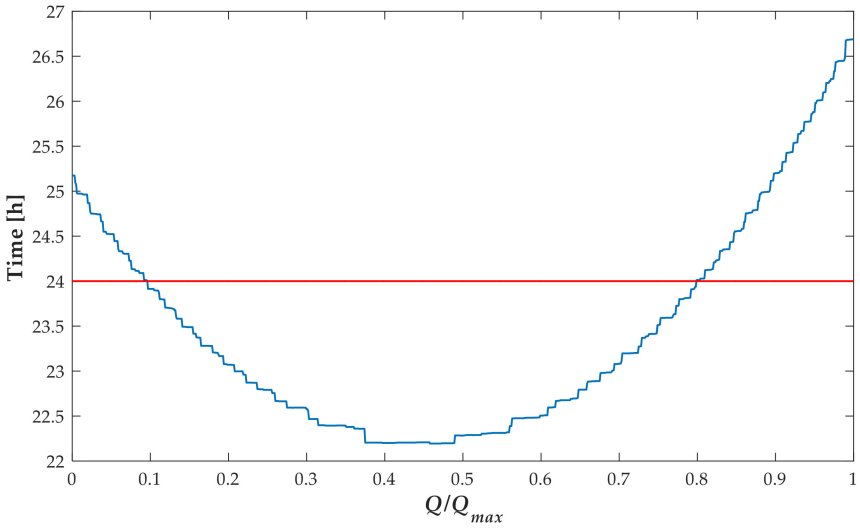

Figure 12. Change in daily transformer aging in function of reactive power factor of the EVCS.

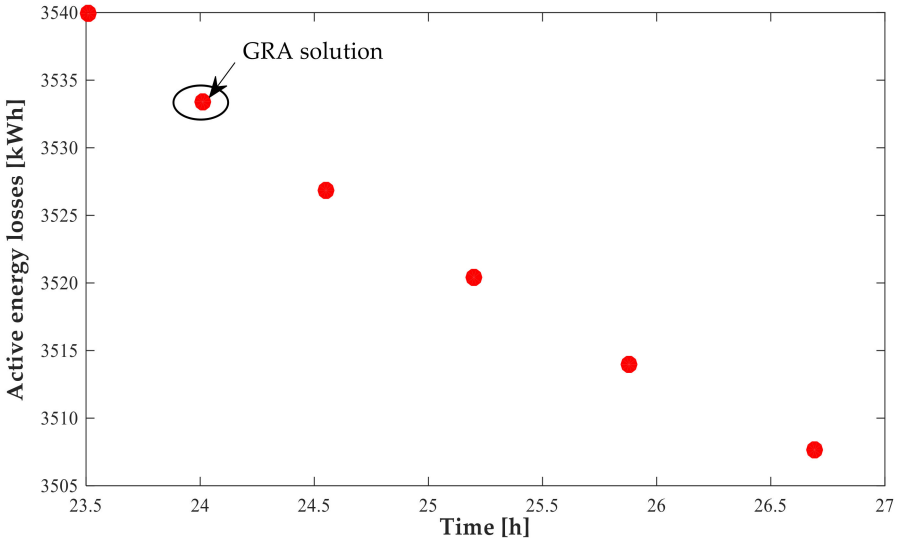

Figure 13. Pareto front optimal solutions.

In order to choose the final solution, a post-optimized analysis based on GRA has been performed. In this paper, the total number of sequences compared equals to the number of optimal solutions obtained by analysed Pareto front solutions. The elements of the sequence are the values of two criteria functions. The results from the GRA analysis are shown in Table 8, the while the optimal solution is pointed out in Figure 13.

Table 8. Obtained Γ_{0i} for the set of optimal solutions.

Daily Transformer Aging [h]	Active Daily Power Losses [kWh]	Q/Q_{max}	Γ_{0i}	Ranking Solution
24.000	3540.0	0.75	0.66667	2
24.012	3533.4	0.80	0.68824	1
24.553	3526.9	0.85	0.58257	4
25.200	3520.4	0.90	0.54352	6
25.880	3514.0	0.95	0.56736	5
26.689	3507.7	1.00	0.66667	2

A set of Pareto front optimal solutions, with points, is shown in Figure 12. For the selected solutions, it is shown that for the analyzed range of reactive power injection, the reduction of active energy losses leads to a faster aging of the transformer.

The solution involves reactive power injection of $0.8Q_{max}$, which means that the losses of active energy amount to 3533.4 kWh and that the daily aging of the transformer is 24.012 h. In the end, the adopted solution enables the reduction of active daily energy loss in the amount of 3.1%. Furthermore, with these values of reactive power injection, the reduction of transformer LOL amounts to 4% compared to the case when an EV operates with the unit power factor and 10.3% when an EV injects maximum available reactive power Q_{max}.

5. Conclusions

In this paper, the potential of reactive power from OBCs in EVCSs to reduce losses of active energy and the aging of transformers is analyzed in detail. For the analyzed network and the number of EVCSs, it is shown explicitly that the injection of reactive power contributes to a reduc-tion in the active energy losses, but contributes significantly more to the reduction of transformer aging. Namely, for the analyzed IEEE 33 bus distribution network and obtained EVCS demand, it is shown that if on-board EV chargers in EVCSs operate in the capacitive mode and with maximum possible reactive power, the losses of active energy are reduced by 3% compared to the scenario when stations operate with the unit power factor. On the other hand, the impact of reactive injection power on the aging of transformers is significantly more pronounced.

The main contribution of this paper is that it has been shown that a relatively small oversizing of the OBCs enables a significant reduction in transformer aging in addition to the reduction of active energy losses in the system. The proposed methodology is based on generally known models for calculating power flows and the widely used model for transformer aging. It is important to emphasize that the proposed methodology can be applied to any network and any number of EVCSs. Furthermore, the proposed methodology takes into account the stochastic nature of the EVs, using appropriate PDFs and MC simulations.

It is important to point out that the contribution of reactive power from EVs at EVCSs depends on the transformer rating and the EVCS demand. In particular, it was shown that if the EVCS demand is 4% higher than planned, it is possible to prevent additional aging of a 200 kVA transformer by injecting reactive power in the range from $0.154Q_{max}$ to Q_{max}. Furthermore, for a transformer of 250 kVA, for a 40% higher EVCS demand, additional aging of a transformer could be prevented by injecting reactive power in the range from $0.096Q_{max}$ to $0.799Q_{max}$.

For different levels of the EVCS demand, there are different values of improvement in LOL. For example, for the increase in the EVCS demand for 7% 200 kVA transformers, there is an 18% improvement in LOL % in comparison to the case where there is no reactive power injecting from EVs. Moreover, with a 60% increase in the EVCS demand for 250 kVA transformers, for optimal reactive power injection, there is a 23.33% improvement of LOL compared to a case where there is a maximum reactive power injection and a 10.3% improvement when an EV operates with the unit power factor.

Author Contributions: All the authors have contributed equally to this work. All authors have read and agreed to the published version of the manuscript.

Funding: This Ministry of Science and Technological Development, Montenegro.

Acknowledgments: The authors are thankful to the anonymous reviewers for comments that helped us improve the paper content.

Conflicts of Interest: The authors declare no conflict of interest.

References

1. Communication from the Commision to the European Parliment, the Council, the European Economic Social Committee a 7nd the Committee of the Regions—A Roadmap for Moving to a Competitive Low Carbon Economy in 2050. 2011. Available online: https://eravisions.archiv.zsi.at/stocktaking/7.html (accessed on 20 September 2022).
2. Alame, D.; Azzouz, M.; Kar, N. Assessing and Mitigating Impacts of Electric Vehicle Harmonic Currents on Distribution Systems. *Energies* **2020**, *13*, 3257. [CrossRef]

3. Khalid, M.S.; Lin, X.; Zhuo, Y.; Kumar, R.; Rafique, M.K. Impact of Energy Management of Electric Vehicles on Transient Voltage Stability of Microgrid. *World Electr. Veh. J.* **2015**, *7*, 577–588. [CrossRef]
4. Gao, Y. *Assessment of Future Adaptability of Distribution Transformer Population under EV Scenarios*; Univeristy of Manchester: Manchester, UK, 2016.
5. Thermal Performance of Transformers. Available online: https://e-cigre.org/publication/ELT_246_4-thermal-performance-of-transformers (accessed on 7 September 2022).
6. Soleimani, M.; Affonso, C.M.; Kezunovic, M. Transformer Loss of Life Mitigation in the Presence of Energy Storage and PV Generation. In Proceedings of the 2019 IEEE PES Innovative Smart Grid Technologies Europe (ISGT-Europe)), Bucharest, Romania, 29 September–2 October 2019; pp. 1–5.
7. Hong, S.-K.; Lee, S.G.; Kim, M. Assessment and Mitigation of Electric Vehicle Charging Demand Impact to Transformer Aging for an Apartment Complex. *Energies* **2020**, *13*, 2571. [CrossRef]
8. Affonso, C.d.M.; Kezunovic, M. Technical and Economic Impact of PV-BESS Charging Station on Transformer Life: A Case Study. *IEEE Trans. Smart Grid* **2019**, *10*, 4683–4692. [CrossRef]
9. Sanchez, A.; Romero, A.; Rattá, G.; Rivera, S. Smart Charging of PEVs to Reduce the Power Transformer Loss of Life. In Proceedings of the 2017 IEEE PES Innovative Smart Grid Technologies Conference—Latin America (ISGT Latin America), Quito, Ecuador, 20–22 September 2017; pp. 1–6.
10. Konstantinidis, G.; Karapidakis, E.; Paspatis, A. Mitigating the Impact of an Official PEV Charger Deployment Plan on an Urban Grid. *Energies* **2022**, *15*, 1321. [CrossRef]
11. Smith, T.; Garcia, J.; Washington, G. Novel PEV Charging Approaches for Extending Transformer Life. *Energies* **2022**, *15*, 4454. [CrossRef]
12. Hilshey, A.D.; Hines, P.D.H.; Rezaei, P.; Dowds, J.R. Estimating the Impact of Electric Vehicle Smart Charging on Distribution Transformer Aging. *IEEE Trans. Smart Grid* **2013**, *4*, 905–913. [CrossRef]
13. Paterakis, N.; Pappi, I.; Erdinc, O.; Godina, R.; Rodrigues, E.; Catalão, J. Consideration of the Impacts of a Smart Neighborhood Load on Transformer Aging. *IEEE Trans. Smart Grid* **2015**, *76*, 2793–2802. [CrossRef]
14. Aravinthan, V.; Jewell, W. Controlled Electric Vehicle Charging for Mitigating Impacts on Distribution Assets. *IEEE Trans. Smart Grid* **2015**, *6*, 999–1009. [CrossRef]
15. Leemput, N.; Geth, F.; Van Roy, J.; Büscher, J.; Driesen, J. Reactive Power Support in Residential LV Distribution Grids through Electric Vehicle Charging. *Sustain. Energy Grids Netw.* **2015**, *3*, 24–35. [CrossRef]
16. Gao, X.; De Carne, G.; Langwasser, M.; Liserre, M. Online Load Control in Medium Voltage Grid by Means of Reactive Power Modification of Fast Charging Station. In Proceedings of the 2019 IEEE Milan PowerTech, Milan, Italy, 23–27 June 2019; pp. 1–6.
17. Wu, C.; Mohsenian-Rad, H.; Huang, J. PEV-Based Reactive Power Compensation for Wind DG Units: A Stackelberg Game Approach. In Proceedings of the 2012 IEEE Third International Conference on Smart Grid Communications (SmartGridComm), 5–8 November 2012; pp. 504–509.
18. Mojdehi, M.N.; Ghosh, P. Modeling and Revenue Estimation of EV as Reactive Power Service Provider. In Proceedings of the 2014 IEEE PES General Meeting | Conference & Exposition, National Harbor, MD, USA, 27–31 July 2014; pp. 1–5.
19. Injeti, S.K.; Thunuguntla, V.K. Optimal Integration of DGs into Radial Distribution Network in the Presence of Plug-in Electric Vehicles to Minimize Daily Active Power Losses and to Improve the Voltage Profile of the System Using Bio-Inspired Optimization Algorithms. *Prot. Control Mod. Power Syst.* **2020**, *5*, 3. [CrossRef]
20. Jamian, J.J.; Mustafa, M.W.; Mokhlis, H.; Baharudin, M.A. Minimization of Power Losses in Distribution System via Sequential Placement of Distributed Generation and Charging Station. *Arab. J. Sci. Eng.* **2014**, *39*, 3023–3031. [CrossRef]
21. Chippada, D.; Reddy, M.D. Optimal Planning of Electric Vehicle Charging Station along with Multiple Distributed Generator Units. *IJISA* **2022**, *14*, 40–53. [CrossRef]
22. Dharavat, N.; Sudabattula, S.K.; Velamuri, S. Integration of Distributed Generation and Electric Vehicles in a Distribution Network Using Political Optimizer. In Proceedings of the 2021 4th International Conference on Recent Developments in Control, Automation & Power Engineering (RDCAPE), Noida, India, 7–8 October 2021; pp. 521–525.
23. Velamuri, S.; Cherukuri, S.H.C.; Sudabattula, S.K.; Prabaharan, N.; Hossain, E. Combined Approach for Power Loss Minimization in Distribution Networks in the Presence of Gridable Electric Vehicles and Dispersed Generation. *IEEE Syst. J.* **2022**, *16*, 3284–3295. [CrossRef]
24. Chang, R.-F.; Chang, Y.-C.; Lu, C.-N. Loss Minimization of Distribution Systems with Electric Vehicles by Network Reconfiguration. In Proceedings of the 2012 International Conference on Control Engineering and Communication Technology, Shenyang, China, 7–9 December 2012; pp. 551–555.
25. Wang, J.; Wang, W.; Wang, H.; Zuo, H. Dynamic Reconfiguration of Multiobjective Distribution Networks Considering DG and EVs Based on a Novel LDBAS Algorithm. *IEEE Access* **2020**, *8*, 216873–216893. [CrossRef]
26. Reddy, M.S.K.; Selvajyothi, K. Optimal Placement of Electric Vehicle Charging Stations in Radial Distribution System along with Reconfiguration. In Proceedings of the 2019 IEEE 1st International Conference on Energy, Systems and Information Processing (ICESIP), Chennai, India, 4–6 July 2019; pp. 1–6.
27. Melo, D.F.R.; Leguizamon, W.; Massier, T.; Beng Gooi, H. Optimal Distribution Feeder Reconfiguration for Integration of Electric Vehicles. In Proceedings of the 2017 IEEE PES Innovative Smart Grid Technologies Conference—Latin America (ISGT Latin America), Quito, Ecuador, 20–22 September 2017; pp. 1–6.

28. Reddy, M.S.K.; Panigrahy, A.K.; Selvajyothi, K. Minimization of Electric Vehicle Charging Stations Influence on Unbalanced Radial Distribution System with Optimal Reconfiguration Using Particle Swarm Optimization. In Proceedings of the 2021 International Conference on Sustainable Energy and Future Electric Transportation (SEFET), Hyderabad, India, 21–23 January 2021; pp. 1–6.
29. Wang, C.; Dunn, R.; Lian, B. Power Loss Reduction for Electric Vehicle Penetration with Embedded Energy Storage in Distribution Networks. In Proceedings of the 2014 IEEE International Energy Conference (ENERGYCON), Cavtat, Croatia, 13–16 May 2014; pp. 1417–1424.
30. Yang, Y.; Zhang, W.; Jiang, J.; Huang, M.; Niu, L. Optimal Scheduling of a Battery Energy Storage System with Electric Vehicles' Auxiliary for a Distribution Network with Renewable Energy Integration. *Energies* **2015**, *8*, 10718–10735. [CrossRef]
31. Acha, S.; Green, T.C.; Shah, N. Effects of Optimised Plug-in Hybrid Vehicle Charging Strategies on Electric Distribution Network Losses. In Proceedings of the IEEE PES T&D 2010, New Orleans, LA, USA, 19–22 April 2010; pp. 1–6.
32. Sortomme, E.; Hindi, M.M.; MacPherson, S.D.J.; Venkata, S.S. Coordinated Charging of Plug-In Hybrid Electric Vehicles to Minimize Distribution System Losses. *IEEE Trans. Smart Grid* **2011**, *2*, 198–205. [CrossRef]
33. Sinha, R.; Moldes, E.; Zaidi, A.; Mahat, P.; Pillai, J.; Hansen, P. An Electric Vehicle Charging Management and Its Impact on Losses. In Proceedings of the IEEE PES ISGT Europe 2013, Lyngby, Denmark, 6–9 October 2013; pp. 1–5.
34. Nafisi, H.; Agah, S.M.M.; Askarian Abyaneh, H.; Abedi, M. Two-Stage Optimization Method for Energy Loss Minimization in Microgrid Based on Smart Power Management Scheme of PHEVs. *IEEE Trans. Smart Grid* **2016**, *7*, 1268–1276. [CrossRef]
35. Rajesh, P.; Shajin, F.H. Optimal Allocation of EV Charging Spots and Capacitors in Distribution Network Improving Voltage and Power Loss by Quantum-Behaved and Gaussian Mutational Dragonfly Algorithm (QGDA). *Electr. Power Syst. Res.* **2021**, *194*, 107049. [CrossRef]
36. Suresh, V.; Sudabattula, S.; Cherukuri, S.H.C. Coordinated Power Loss Minimization Technique for Distribution Systems in the Presence of Electric Vehicles. In Proceedings of the 2019 National Power Electronics Conference (NPEC), Tiruchirappalli, India, 13–15 December 2019; pp. 1–5.
37. IEEE SA—IEEE C57.91-2011. Available online: https://standards.ieee.org/ieee/C57.91/5297/ (accessed on 10 August 2022).
38. Waseem, M.; Sajjad, I.A.; Haroon, S.S.; Amin, S.; Farooq, H.; Martirano, L.; Napoli, R. Electrical Demand and Its Flexibility in Different Energy Sectors. *Electr. Power Compon. Syst.* **2020**, *48*, 1339–1361. [CrossRef]
39. Abdelaziz, A.Y.; Hegazy, Y.G.; El-Khattam, W.; Othman, M.M. A Multi-Objective Optimization for Sizing and Placement of Voltage-Controlled Distributed Generation Using Supervised Big Bang–Big Crunch Method. *Electr. Power Compon. Syst.* **2015**, *43*, 105–117. [CrossRef]
40. Mo, T.; Li, Y.; Lau, K.-t.; Poon, C.; Wu, Y.; Luo, Y. Trends and Emerging Technologies for the Development of Electric Vehicles. *Energies* **2022**, *15*, 6271. [CrossRef]
41. Ravi, S.; Aziz, M. Utilization of Electric Vehicles for Vehicle-to-Grid Services: Progress and Perspectives. *Energies* **2022**, *15*, 589. [CrossRef]
42. Germanà, R.; Liberati, F.; De Santis, E.; Giuseppi, A.; Delli Priscoli, F.; Di Giorgio, A. Optimal Control of Plug-In Electric Vehicles Charging for Composition of Frequency Regulation Services. *Energies* **2021**, *14*, 7879. [CrossRef]
43. Neofytou, N.; Blazakis, K.; Katsigiannis, Y.; Stavrakakis, G. Modeling Vehicles to Grid as a Source of Distributed Frequency Regulation in Isolated Grids with Significant RES Penetration. *Energies* **2019**, *12*, 720. [CrossRef]
44. Lan, T.; Jermsittiparsert, K.; Alrashood, S.T.; Rezaei, M.; Al-Ghussain, L.; Mohamed, M.A. An Advanced Machine Learning Based Energy Management of Renewable Microgrids Considering Hybrid Electric Vehicles' Charging Demand. *Energies* **2021**, *14*, 569. [CrossRef]
45. Aziz, M.; Oda, T.; Mitani, T.; Watanabe, Y.; Kashiwagi, T. Utilization of Electric Vehicles and Their Used Batteries for Peak-Load Shifting. *Energies* **2015**, *8*, 3720–3738. [CrossRef]
46. Tovilović, D.M.; Rajaković, N.L.J. The Simultaneous Impact of Photovoltaic Systems and Plug-in Electric Vehicles on the Daily Load and Voltage Profiles and the Harmonic Voltage Distortions in Urban Distribution Systems. *Renew. Energy* **2015**, *76*, 454–464. [CrossRef]
47. Deilami, S.; Masoum, A.; Moses, P.; Masoum, M. Real-Time Coordination of Plug-In Electric Vehicle Charging in Smart Grids to Minimize Power Losses and Improve Voltage Profile. Smart Grid. *IEEE Trans. Smart Grid* **2011**, *2*, 456–467. [CrossRef]
48. Khatiri-Doost, S.; Amirahmadi, M. Peak Shaving and Power Losses Minimization by Coordination of Plug-in Electric Vehicles Charging and Discharging in Smart Grids. In Proceedings of the 2017 IEEE International Conference on Environment and Electrical Engineering and 2017 IEEE Industrial and Commercial Power Systems Europe (EEEIC/I&CPS Europe), Milan, Italy, 6–9 June 2017; pp. 1–5.
49. Wang, J.; Bharati, G.R.; Paudyal, S.; Ceylan, O.; Bhattarai, B.P.; Myers, K.S. Coordinated Electric Vehicle Charging With Reactive Power Support to Distribution Grids. *IEEE Trans. Ind. Inf.* **2019**, *15*, 54–63. [CrossRef]
50. Kisacikoglu, M.C. *Vehicle-to-Grid (V2G) Reactive Power Operation Analysis of the EV/PHEV Bidirectional Battery Charger*; Univeristy of Tennessee: Knoxville, TN, USA, 2013.
51. *IEEE Standards 519-1992*; IEEE Recommended Practices and Requirements for Harmonic Control in Electrical Power Systems. InSMute of Elmeal and Ehxtronics Engineers, Inc.: New York, NY, USA, 1993; pp. 1–112. [CrossRef]
52. *IEEE Standards 1547-2003*; IEEE Standard for Interconnecting Distributed Resources with Electric Power Systems. InSMute of Elmeal and Ehxtronics Engineers, Inc.: New York, NY, USA, 2003; pp. 1–28. [CrossRef]

53. Xu, D.; Pei, W.; Zhang, Q. Optimal Planning of Electric Vehicle Charging Stations Considering User Satisfaction and Charging Convenience. *Energies* **2022**, *15*, 5027. [CrossRef]
54. Campaña, M.; Inga, E.; Cárdenas, J. Optimal Sizing of Electric Vehicle Charging Stations Considering Urban Traffic Flow for Smart Cities. *Energies* **2021**, *14*, 4933. [CrossRef]
55. Baik, S.H.; Jin, Y.G.; Yoon, Y.T. Determining Equipment Capacity of Electric Vehicle Charging Station Operator for Profit Maximization. *Energies* **2018**, *11*, 2301. [CrossRef]
56. Flammini, M.G.; Prettico, G.; Julea, A.; Fulli, G.; Mazza, A.; Chicco, G. Statistical Characterisation of the Real Transaction Data Gathered from Electric Vehicle Charging Stations. *Electr. Power Syst. Res.* **2019**, *166*, 136–150. [CrossRef]
57. Sanna, L. Driving the Solution the Plug-in Hybrid Electric Vehicle. *EPRI J.* **2005**, *1*, 8–17.
58. Mohamed, A.; Salehi, V.; Ma, T.; Mohammed, O. Real-Time Energy Management Algorithm for Plug-In Hybrid Electric Vehicle Charging Parks Involving Sustainable Energy. *IEEE Trans. Sustain. Energy* **2014**, *5*, 577–586. [CrossRef]
59. EV-Volumes—The Electric Vehicle World Sales Database. Available online: https://www.ev-volumes.com/ (accessed on 10 August 2022).
60. Worldwide Electric Vehicle Sales by Model. 2021. Available online: https://www.statista.com/statistics/960121/sales-of-all-electric-vehicles-worldwide-by-model/ (accessed on 10 August 2022).
61. Grunditz, E.A.; Thiringer, T. Performance Analysis of Current BEVs Based on a Comprehensive Review of Specifications. *IEEE Trans. Transp. Electrif.* **2016**, *2*, 270–289. [CrossRef]
62. De Freige, M.; Ross, M.; Joos, G.; Dubois, M. Power & Energy Ratings Optimization in a Fast-Charging Station for PHEV Batteries. In Proceedings of the 2011 IEEE International Electric Machines & Drives Conference (IEMDC), Niagara Falls, ON, Canada, 15–18 May 2011; pp. 486–489.
63. Kawambwa, S.; Mwifunyi, R.; Mnyanghwalo, D.; Hamisi, N.; Kalinga, E.; Mvungi, N. An Improved Backward/Forward Sweep Power Flow Method Based on Network Tree Depth for Radial Distribution Systems. *J. Electr. Syst. Inf. Technol.* **2021**, *8*, 7. [CrossRef]
64. Ghosh, S.; Das, D. Method of Load Flow Solution of Radial Distribution Network. *Gener. Transm. Distrib. IEE Proc.* **1999**, *146*, 641–648. [CrossRef]
65. Rizwan, M.; Waseem, M.; Liaqat, R.; Sajjad, I.A.; Dampage, U.; Salmen, S.H.; Obaid, S.A.; Mohamed, M.A.; Annuk, A. SPSO Based Optimal Integration of DGs in Local Distribution Systems under Extreme Load Growth for Smart Cities. *Electronics* **2021**, *10*, 2542. [CrossRef]
66. Waseem, M.; Lin, Z.; Liu, S.; Zhang, Z.; Aziz, T.; Khan, D. Fuzzy Compromised Solution-Based Novel Home Appliances Scheduling and Demand Response with Optimal Dispatch of Distributed Energy Resources. *Appl. Energy* **2021**, *290*, 116761. [CrossRef]
67. Waseem, M.; Lin, Z.; Liu, S.; Sajjad, I.A.; Aziz, T. Optimal GWCSO-Based Home Appliances Scheduling for Demand Response Considering End-Users Comfort. *Electr. Power Syst. Res.* **2020**, *187*, 106477. [CrossRef]
68. Abdmouleh, Z.; Gastli, A.; Ben-Brahim, L.; Haouari, M.; Al-Emadi, N.A. Review of Optimization Techniques Applied for the Integration of Distributed Generation from Renewable Energy Sources. *Renew. Energy* **2017**, *113*, 266–280. [CrossRef]
69. Smart City—INVEST IN PODGORICA. Available online: http://investinpodgorica.me/?page_id=1040 (accessed on 18 September 2022).
70. Rubinstein, R.Y.; Kroese, D.P. *Simulation and the Monte Carlo Method*, 3rd ed.; Wiley Series in Probability and Statistics; John Wiley & Sons, Inc.: Hoboken, NJ, USA, 2017; ISBN 978-1-118-63220-8.
71. Malekpoor, H.; Chalvatzis, K.; Mishra, N.; Mehlawat, M.K.; Zafirakis, D.; Song, M. Integrated Grey Relational Analysis and Multi Objective Grey Linear Programming for Sustainable Electricity Generation Planning. *Ann. Oper. Res.* **2018**, *269*, 475–503. [CrossRef]
72. Durković, V.; Savić, A.S. ATC Enhancement Using TCSC Device Regarding Uncertainty of Realization One of Two Simultaneous Transactions. *Int. J. Electr. Power Energy Syst.* **2020**, *115*, 105497. [CrossRef]
73. Xu, G.; Yang, Y.; Lu, S.; Li, L.; Song, X. Comprehensive Evaluation of Coal-Fired Power Plants Based on Grey Relational Analysis and Analytic Hierarchy Process. *Energy Policy* **2011**, *39*, 2343–2351. [CrossRef]
74. Liu, G.; Baniyounes, A.; Rasul, M.; Than Oo, A.; Khan, M.M. General Sustainability Indicator of Renewable Energy System Based on Grey Relational Analysis. *Int. J. Energy Res.* **2013**, *37*, 1928–1936. [CrossRef]
75. Dharageshwari, K.; Nayanatara, C. Multiobjective Optimal Placement of Multiple Distributed Generations in IEEE 33 Bus Radial System Using Simulated Annealing. In Proceedings of the 2015 International Conference on Circuits, Power and Computing Technologies [ICCPCT-2015], Nagercoil, India, 19–20 March 2015; pp. 1–7.
76. Karadimos, D.I.; Karafoulidis, A.D.; Doukas, D.I.; Gkaidatzis, P.A.; Labridis, D.P.; Marinopoulos, A.G. Techno-Economic Analysis for Optimal Energy Storage Systems Placement Considering Stacked Grid Services. In Proceedings of the 2017 14th International Conference on the European Energy Market (EEM), Dresden, Germany, 6–9 June 2017; pp. 1–6.
77. Chen, C.-S.; Wu, T.-H. Optimal Distribution Transformer Sizing by Dynamic Programming. *Int. J. Electr. Power Energy Syst.* **1998**, *20*, 161–167. [CrossRef]
78. Aravinthan, V.; Argade, S. Optimal Transformer Sizing with the Presence of Electric Vehicle Charging. In Proceedings of the 2014 IEEE PES T&D Conference and Exposition, Chicago, IL, USA, 14–17 April 2014; pp. 1–5.